Available online at www.sciencedirect.com
SCIENCE DIRECT®
Journal of Power Sources 126 (2004) 193–202
JOURNAL OF POWER SOURCES
www.elsevier.com/locate/jpowsour

Li-ion microbatteries generated by a laser direct-write method

Ryan Wartena [a], Aimee E. Curtright [a], Craig B. Arnold [b], Alberto Piqué [b], Karen E. Swider-Lyons [a,*]

[a] *Surface Chemistry Branch, Code 6171, Naval Research Laboratory, Washington, DC 20375-5342, USA*
[b] *Surface Modification Branch, Code 6372, Naval Research Laboratory, Washington, DC 20375-5342, USA*

Received 25 July 2003; accepted 22 August 2003

Abstract

A laser-based direct-write process is demonstrated as a method to fabricate Li-ion microbatteries. The battery electrodes are made by the laser-induced forward transfer of inks of charge-storage materials (composites of carbon/binder and $LiCoO_2$/carbon/binder) onto micromachined metal-foil current collectors to form 40–60 μm thick electrodes with 16 mm^2 (4 mm × 4 mm) footprints. Both half cells and packaged microbatteries display capacities of approximately 155 μAh or 100 mAh/g, as normalized to the amount of $LiCoO_2$, and are comparable to the capacities of control electrodes that have been stenciled and pressed. The electrode capacities are not compromised when they are assembled into microbatteries, packaged and tested in air. The density and volumetric capacity of the laser-transferred electrodes are lower than those reported for sputtered thin-film microbatteries, yet the former electrodes can be made thicker and therefore deliver the same amount of charge from a smaller footprint. The data indicate that this laser direct-write method may be a viable approach for developing Li-ion microbattery systems for autonomous microelectronic devices and microsensors.

Keywords: Microbattery; Battery; Li-ion; Direct-write; Laser

1. Introduction

A current trend in technology is towards the deployment of autonomous microdevices and microsensors, and batteries are likely to be either the sole power source or a component in a hybrid power source for these new electronics systems [1,2]. Although batteries have relatively low specific energies and power compared to that promised by fuel cells and engines, respectively, batteries have significant advantages in that their chemistry is fairly well understood. They have no moving parts or fluids, so their miniaturization is straightforward. Batteries are also less hazardous as they become smaller because issues such as runaway heating are minimized. Because batteries have a low heat signature and generate no noise, they cause little physical disruption to microelectronic systems.

Another advantage of using microbatteries for micropower sources is the opportunity for direct integration into electronic components. A battery incorporated into an electronics circuit saves weight by using the electronics substrate as the battery packaging. Co-locating the battery with electronic components also reduces the weight of and ohmic losses along interconnects. Microbatteries can also be used as the voltage source for piezoelectric converters in microdevices [3]. Furthermore, the μW-level power of microbatteries matches well to that of solar and radio frequency (RF) energies, making them well suited as charge-storage media for energy-harvesting systems.

There have been numerous efforts to make Li and Li-ion microbatteries utilizing methods compatible with microprocessing, including sputtering and lithography techniques [4]. Sputtering methods have been applied extensively [5,6], as they can deposit all the necessary cell components including current collectors (Cu and Al), electrolyte/separator (usually lithium phosphorous oxynitride, LiPON), positive electrodes ($LiCoO_2$ or $LiMn_2O_4$), and negative electrodes (Li-metal). RF magnetron sputtering has been used to deposit lithium silicon tin oxynitride (Li_ySiTON) as a negative electrode material, which was then combined with a sputtered LiPON separator and $LiCoO_2$-positive electrode to produce a Li-ion microbattery [7]. A similar approach was employed to make V_2O_5/LiPON/LiV_2O_5 batteries on flexible Al foil substrates [8]. Sputtering and sol–gel spin coating methods can be combined to make Li microbattery arrays embedded in Si trenches [9]. These Si-entrenched microbatteries comprise

* Corresponding author. Tel.: +1-202-404-3314; fax: +1-202-767-3321.
E-mail address: karen.lyons@nrl.navy.mil (K.E. Swider-Lyons).

0378-7753/$ – see front matter © 2003 Elsevier B.V. All rights reserved.
doi:10.1016/j.jpowsour.2003.08.019

Al negative current collectors, Li-metal negative electrodes, SiO_2–P_2O_5 electrolytes, $LiMn_2O_4$-positive electrodes, and polycrystalline Si positive current collectors, and they are 100 μm wide, 200 μm long, and 0.5–2 μm deep. Other battery chemistries fabricated with microfabrication techniques include TiS_2/LiI/Li [4] and nickel–zinc [10]. An advantage of these approaches is that they leverage methods from the multi-billion-dollar microprocessing industry. The techniques are also able to control the deposition and thickness of the active layers with precision, and therefore the capacity of the electrodes can be optimized to make an efficient battery with minimal defects. Drawbacks to these approaches are that they cannot be used to deposit conventional composite battery electrodes (active material, carbon, and electrolyte). Because sputtered positive electrodes contain only the semi-conducting active material (e.g. $LiCoO_2$) and no carbon, the thickness of the electrode must be limited to several microns to keep the cell resistance low, which thereby limits the capacity of the battery. Furthermore, after deposition, the battery materials often need to undergo phase transformations at temperatures higher than is practical for silicon and other substrates, and vacuum conditions often prevent the use of volatile materials. Additionally, the modification of microfabrication designs can be time and labor intensive, and film deposition rates are generally slow (nm to μm/h).

Direct-write techniques are alternative, non-lithographic methods that can be used for microbattery fabrication. The term “direct-write” encompasses a range of methods by which materials on a substrate are modified with an electron, X-ray or light beam, or the materials are printed directly onto a substrate via a probe or forward transfer process [11]. This manuscript focuses on a laser-based direct-write technique that utilizes the laser-forward transfer of materials in a given pattern onto a substrate. The method was originally coined as the matrix-assisted pulsed laser evaporation direct-write process, or MAPLE DW, and was developed for the fabrication of electronic components and sensors [12,13]. MAPLE DW is described as a soft laser-transfer process because there is minimal interaction of the laser with the material being transferred [11–14]. Because the process can be carried out in ambient temperature and pressure conditions, temperature-sensitive and corrosive charge-storage materials can be utilized, as has been successfully demonstrated for the creation of hydrous RuO_2 ultracapacitors in a sulfuric acid electrolyte [15]. The process has the additional feature of laser micromachining, which is useful for creating current collectors, and can be used to carve electrodes of various dimensions, therefore allowing the flexibility to prototype and produce power systems/sources that are tailored to provide optimum power/energy to a particular microelectronic device [1,15].

A schematic illustration of how the laser direct-write process is used to make the Li-battery electrodes is shown in Fig. 1. The details of the method have been described in detail elsewhere [14–17], but a summary is given herein. First, high purity metal foils are micromachined into a desired shape to serve as current collectors. Next, the materials to be deposited are prepared as inks that contain powder (e.g. active material, carbon, binder) and an organic liquid and then cast onto a transparent glass plate, or “ribbon”. The ribbon is mounted over the current collector, and then a pulsed laser is used to forward transfer the ink from the ribbon onto the metal foil. It is understood that the laser evaporates a small amount of the organic liquid, and this instantaneously creates a gas bubble that moves a micron-sized droplet of ink from the ribbon onto the substrate. The volume of the ink droplet is proportional to the width of the laser beam and the thickness of the ink on the ribbon. The composition of the ink formulation is adjusted by varying the size of the particulate matter and the type and amount of solvent to achieve optimum transfer properties. The fluence of the laser also has an impact on how well the ink is transferred. The ribbon and substrate are rastered during the deposition process by computer-controlled *X*–*Y* translation stages. A pad or other design is written or printed on the substrate by

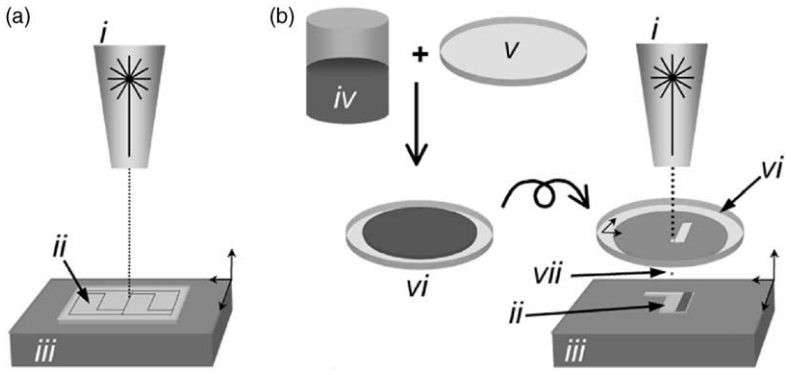

Fig. 1. Schematic illustration of how the laser direct-write apparatus (11–17) is used to create Li-ion battery electrodes. (a) A laser (i) is used to micromachine current collectors (ii) from metal foil. The foil is mounted on a computer-controlled translation stage (iii). (b) An ink comprising active battery materials, binder and an organic liquid (iv) is coated onto a UV-transparent plate (v) to form a ribbon (vi). The ink is then laser-forward transferred from the ribbon to the current collector in a succession of droplets (vii). Both the ribbon and current collector are moved as the material is deposited to build a pad of desired size and thickness.

the cumulative laser transfer of thousands of ink droplets, and several layers of ink can be transferred on top of each other to build a thicker pad. The use of a high-frequency laser allows writing speeds up to 1 m/s. The substrate can be subsequently heated to remove any residual organic liquid, leaving behind a solid pad on the substrate.

The viability of this laser direct-write method for Li-ion microbattery fabrication is demonstrated by creating positive and negative electrodes, and then testing their performance in half cells and full microbatteries [16]. The size and shape of the microbattery electrodes are arbitrarily chosen to be a 4 mm × 4 mm square, although this direct-write approach could be used to produce batteries with features as small as 10 μm and in different geometries. The negative electrodes comprise a carbon composite, the positive electrodes a $LiCoO_2$ composite, and the current collectors are laser-machined Cu and Al foils. A layer of carbon and a polymeric binder is deposited on the current collectors prior to the deposition of the active materials to reduce ohmic losses in the cells by improving contact between the electrode material and the substrate. The Li-ion electrodes are evaluated for their electrochemical performance under half-cell and battery operating conditions, and their capacity is validated by comparison to control electrodes. After cycling as half cells, the electrodes are assembled into microbatteries, packaged and then operated in ambient air. Additionally, cells are constructed from freshly deposited electrodes (that have not been first cycled in half cells) to demonstrate the possibility of a manufacturing sequence compatible with making "a battery on a chip".

2. Experimental

The electrodes for direct-write Li-ion microbatteries are created according to Fig. 1. Aluminum and copper foils (All-Foils, Inc.) for the positive and negative electrodes, respectively, are laser micromachined with a pulsed Nd:YAG laser (355 nm) using a 10–20 μm beam spot into a flag shape having a 4 mm × 4 mm square and a 1 mm × 6 mm shaft. After cutting, the surface of the current collectors are roughened with a 220 grit silicon carbide paper, washed in acetone/methanol, and vacuum dried, in order to improve adhesion and remove surface oxides. Whereas micromachined foils could not be used for the current collectors of a directly integrated power source, their use is appropriate for this first demonstration of a laser direct-write Li-ion microbattery.

The materials composition of the inks is similar to that of conventional carbon-negative and $LiCoO_2$-positive electrodes. The ink for the positive electrode contains a mixture of 89 wt.% 10 μm $LiCoO_2$ particles, 7% carbon (2% Super P; Ensaco and 5% KS6; Timcal) and 4% polyvinylidene fluoride (PVDF; Atofina). An equal weight of 1-methyl-2 pyrrolidone (NMP; Aldrich) is added to the powder. The ink for the negative electrode consists of 91% ≤25 μm diameter carbon (mesoporous carbon microbeads, MCMB 25–28; Alumina Trading Co.) and 2% Super P and 7% PVDF. The weight of NMP in the negative electrode ink is twice than that of the powder. The ink for the adhesion layer comprises 10% Super P and 90% PVDF mixed with 10× their weight in NMP. The inks are laser transferred from the ribbon to the 4 mm × 4 mm area of the current collector by the Nd:YAG laser with a 120 μm beam spot and a fluence between 0.03 and 0.1 J/cm^2. A single layer of the ink for the adhesion layer is deposited directly on the Al and Cu foil current collectors, dried on a hot plate and weighed. Next, a pad of $LiCoO_2$ or carbon ink is built up on the adhesion layer. Two to five layers of ink are added on top of each other to increase the amount of active material in the electrode. After the active materials have been transferred, the electrodes are dried on a hot plate for less than 1 min, vacuum dried at 90–95 °C for 12 h, and then transferred to an Ar glove box.

Control electrodes (non-laser-transferred) are made by a stenciling process. Stencils are created by cutting 4 mm × 4 mm squares out of a 120 μm thick polyimide sheet (Kapton; DuPont). A stencil is placed over the appropriate Al or Cu current collector, and then its well is filled via pipet with the same electrode ink described above for the laser process. As for the laser-transferred electrodes, a conductive coating layer is deposited first on the current collector. The ink is made level with the top plane of the stencil using edge of a razor blade, and then the stencil is peeled away leaving a wet pad having approximately the thickness of the polyimide sheet. The stenciled electrode is then heated under vacuum at 90 °C and then pressed at 3000 psi for 1 min. Control electrodes are chosen for comparison to the laser-transferred electrodes based on their mass.

The physical and morphological attributes of selected control and laser-transferred electrodes are evaluated by profilometry (KLA-Tencor), X-ray diffraction (Cu Kα radiation; Bruker D8 Advance), scanning electron microscopy (LEO 1550) and optical microscopy (Olympus).

Microbatteries are made by two protocols. With the first method, the electrodes are charged and discharged in half cells in open (excess) electrolyte to determine the capacities of the individual electrode before they are assembled into full cells and packaged [17]. Alternatively, the electrodes are directly packaged with electrolyte (with no half-cell cycling) to mimic the conditions that the electrodes would experience in a fabrication process. Microbatteries are made by placing the electrodes on either side of a porous polymer sheet (Celgard 2730) and then by impulse sealing the ensemble within a clear solid polymer (Saranex SX 23-P) that serves as an inner bag. The electrode/separator/inner bag is then impulse-sealed within a pouch of a tri-layer polyethylene–Al–polyester film. The microbattery is filled with 20–60 μl of 1 M $LiPF_6$/carbonate (ethylene carbonate/propylene carbonate/ethyl methyl carbonate/diethyl carbonate) electrolyte via syringe through holes in the inner and outer bags, which are subsequently closed by impulse sealing.

Chronopotentiometry of the half-cell electrodes is carried out at an approximate rate of C/5 (charge and discharge current) using a battery tester (Maccor 2300), which corresponds to current densities between 0.21 and 0.8 mA/cm^2 (or 34–128 μA). The half-cell measurements utilize a Li-foil (Li/Li$^+$) reference electrode and Li-foil counter electrode in ∼20 ml of electrolyte. The electrodes are aligned with 1 cm of electrolyte between them and soaked for 12–24 h before electrochemical evaluation. Carbon-negative electrodes are cycled between 1 and 0.05 V vs. Li/Li$^+$, and $LiCoO_2$-positive electrodes are cycled between 3 and 4.17 V vs. Li/Li$^+$ without rest periods between charge and discharge cycles. The full cells in open electrolyte are operated between 3 and 4.17 V using a three-electrode cell configuration with a carbon-negative electrode, a $LiCoO_2$-positive electrode, and a Li/Li$^+$ reference electrode. After the full cells are assembled into microbatteries, two-electrode measurements are made in the Ar glove box before testing in ambient conditions. All full-cell cycling data are presented as the cell voltage, which is the potential difference between the positive and negative electrodes.

The absolute capacity of the electrodes is reported in μAh. The specific capacity (mAh/g) is calculated from the absolute capacity and the amount of active materials in the electrode. The active material is calculated from the weights of the electrodes before and after the laser-transfer process minus the weights of the inactive materials. The Super P in the adhesion layer is also included when calculating the mass of the active materials in the negative electrode. All mass measurements are carried out in air using a microbalance (Sartorius). The calculations assume that the percentage of active material in the laser-transferred electrode is the same as that in the starting ink, and that none of the organic vehicle remains after the electrodes are dried. The microbattery is described by its footprint or geometric area and mass of $LiCoO_2$ in the positive electrode so that capacities may be compared across half-cell and full-cell measurements.

3. Results

Profilometry experiments indicate that the laser-transferred adhesive/conductive layers have average heights of 30 ± 3 μm. The laser-transferred positive and negative electrode pads on top of the conductive layers have average heights of 40 ± 3 and 60 ± 20 μm, respectively. The variation in the heights of the pads is comparable to the size of the particles used in the battery electrode inks.

Optical micrographs of laser-transferred and control carbon-negative electrodes are shown in Figs. 2a and b, respectively. The electrodes are visually equivalent, as the carbon particles appear to have similar size and shapes in the two samples. The $LiCoO_2$ in the laser-transferred positive electrode (Fig. 2c) also appears to be similar in size and distribution to the control sample (Fig. 2d). SEM images show that the grains of $LiCoO_2$ retain their size and faceted shape indicating that the laser-transfer process does not melt or break apart the $LiCoO_2$ grains. Likewise, X-ray

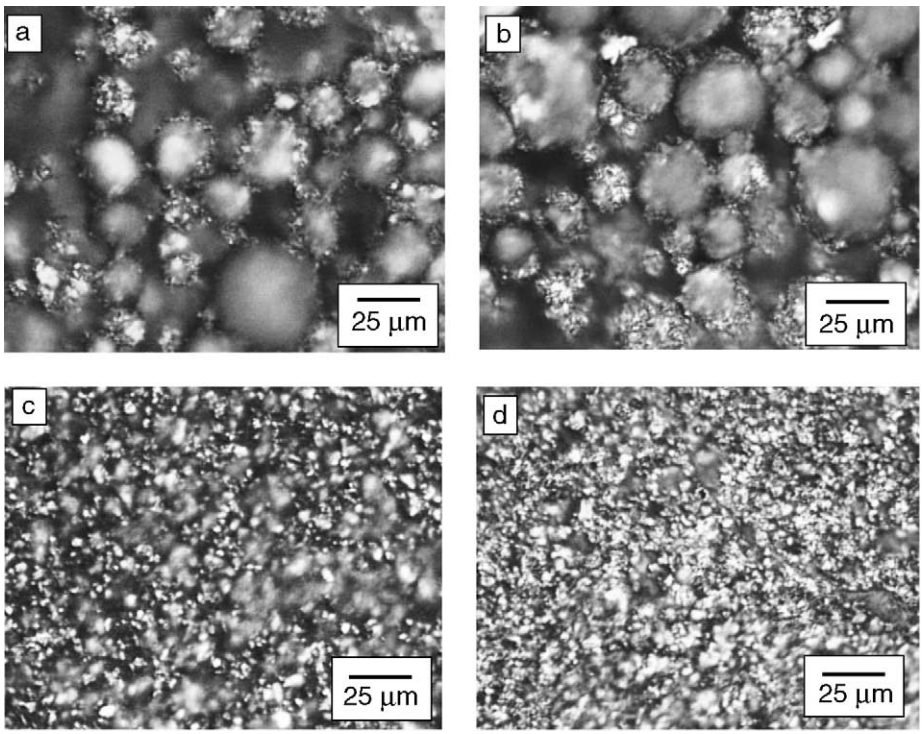

Fig. 2. Optical micrograph comparison of (a) a laser-transferred carbon electrode, (b) a control (stenciled) carbon electrode, (c) a laser-transferred $LiCoO_2$ electrode, and (d) a control (stenciled) $LiCoO_2$ electrode.

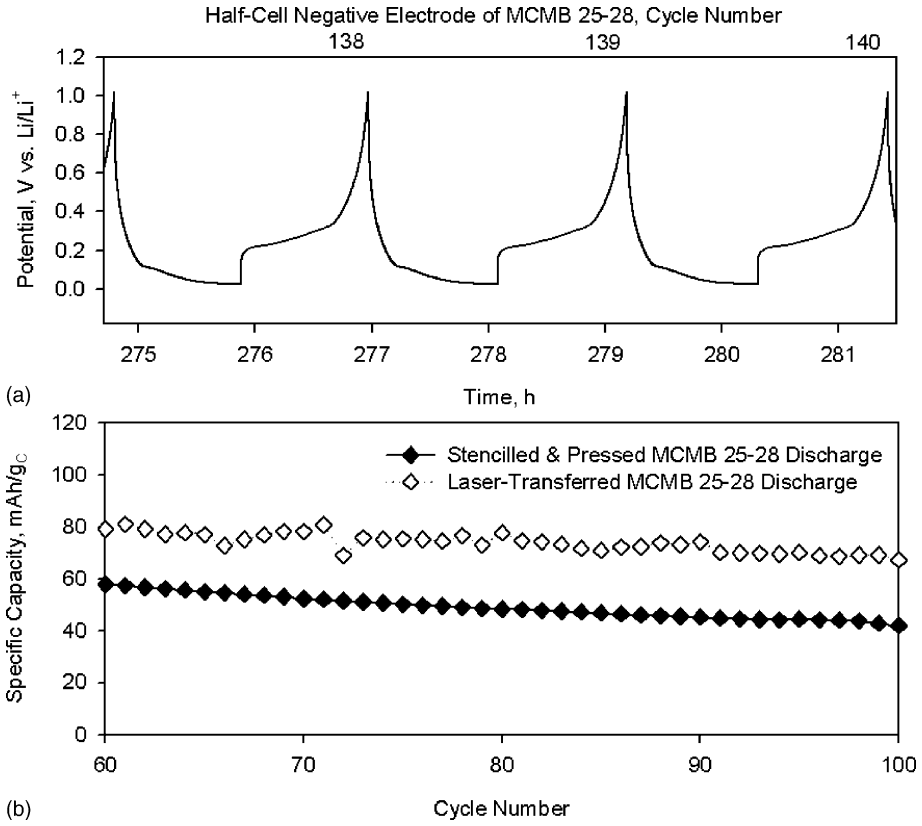

Fig. 3. (a) Charge and discharge data for cycles 138–140 of a laser-transferred carbon electrode in a half cell vs. Li/Li^+ in a 1 M $LiPF_6$/carbonate electrolyte in an Ar glove box. (b) Comparison of the capacities of a laser-transferred carbon electrode (open diamonds) to a control carbon electrode (closed diamonds). The capacities are summarized in Table 1.

diffraction patterns of the positive electrodes indicate that laser-transferred and control electrodes are both oriented normal to the (0 0 3) crystal habit of the as-received $LiCoO_2$ powders, so the lack of mechanical pressure in the laser direct-write process does not cause significant deviations in the electrode morphology.

Half-cell measurements show that the laser-transferred carbon and $LiCoO_2$ electrodes have the expected charge and discharge profiles with plateaus around 0.3 and 3.7 V vs. Li/Li^+, respectively (Figs. 3a and 4a). The specific capacities of electrodes made by laser direct-write and stenciling are illustrated in Fig. 3b (carbon) and Fig. 4b ($LiCoO_2$), while their weights, charge–discharge currents, specific capacities, and absolute capacities are enumerated in Table 1. The same electrodes are used throughout Figs. 3–5, yet the cycles and hours in each figure are reset to zero as configurations or environments of the electrodes are changed. All the plots show 31.5 h of data, with the exception of the carbon-negative electrode in Fig. 3a that has a 6.5 h window. Laser-transferred and control electrodes of the carbon have specific capacities of 101 and 178 mAh/g_{Carbon}, respectively, on their first cycle, both of which are lower than the expected 300 mAh/g_{Carbon} [18]. From the 60th to the 100th cycle, the electrodes exhibit

Table 1
Specific capacities (mAh/g) and absolute capacities (μAh) of laser-transferred and control electrodes at various cycles for the two-electrode configuration in open electrolyte in an Ar glove box[a]

Electrode	Mass of active material (mg), active material	Charge (μA) (discharge current, mA/cm^2)	Specific capacity of active material (mAh/g) (absolute capacity, μAh)			
			1st complete cycle	2nd cycle	30th cycle	100^{th} cycle
Negative laser-transferred[b]	2.153, carbon	128 (0.8)	111 (238)	78.2 (168)	35.0 (75.4)	67.2 (145)
Negative stenciled and pressed[b]	0.990, carbon	56.0 (0.35)	178 (176)	131 (129)	81.1 (80.3)	42.0 (41.6)
Positive laser-transferred	1.585, $LiCoO_2$	34.0 (0.21)	115 (183)	112 (179)	97.4 (154)	
Positive stenciled and pressed	1.958, $LiCoO_2$	43.0 (0.27)	90.3 (177)	88.2 (173)	81.4 (159)	

[a] Other specifications such as active material mass and discharge current are also provided. The electrode areas are 4 mm × 4 mm.
[b] MCMB 25–28 carbon.

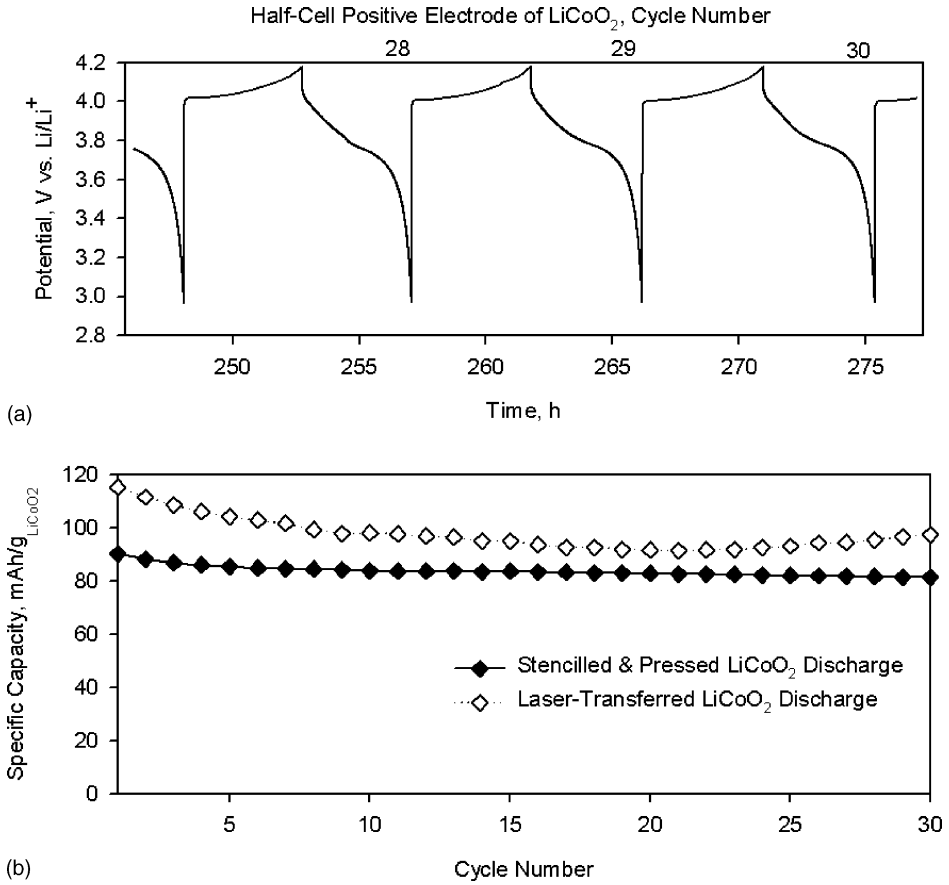

Fig. 4. (a) Charge and discharge data for cycles 28–30 of a laser-transferred $LiCoO_2$-positive electrode vs. Li/Li^+ in a 1 M $LiPF_6$/carbonate electrolyte. (b) Comparison of the specific capacity comparison of a laser-transferred $LiCoO_2$ electrode (open diamonds) to a control $LiCoO_2$ electrode (closed diamonds). The capacities are summarized in Table 1.

comparable specific capacities and fade at similar rates. Other carbon electrodes made by laser direct-write have had specific capacities as high as 183 mAh/g_{Carbon} on the first cycle, indicating that the laser process can make high capacity negative electrodes. Table 1 also shows that the laser-transferred $LiCoO_2$ electrode performs well vs. the control electrode—115 vs. 90.3 mAh/g_{LiCoO_2}, respectively, on the first cycle and 97.4 vs. 81.4 mAh/g_{LiCoO_2}, after 30 cycles at a ~C/5 rate. These values are near the reported capacities of 110–150 mAh/g_{LiCoO_2} for electrodes discharged at C/2–C/20 rates, respectively [18]. The laser-transferred electrodes show no evidence of delamination from the current collectors when the adhesion layer is used.

The absolute capacities of the electrodes (μAh) are used to match electrodes to construct efficient microbatteries. Fig. 5 follows the charge and discharge profiles of a set of positive and negative electrodes having capacities of 154 and 145 μAh, respectively, as they are assembled in full cells, packaged, and finally tested in ambient air. The discharge capacities (specific and absolute) are listed in Table 2. Full cells in an Ar atmosphere and open electrolyte show excellent charging and discharging behavior (Fig. 5a), indicating that the half-cell performances of the individual electrodes are not compromised in full cells due to mismatched electrode capacities. Fig. 5b shows the performance of the same electrodes in an Ar environment when assembled as

Table 2
Specific capacities (mAh/g) and absolute capacities (μAh) of laser-transferred electrodes from Table 1 in full-cell and packaged-battery configurations[a]

System	Charge (μA) (discharge current, mA/cm^2)	Specific capacity of $LiCoO_2$ (mAh/g) (absolute capacity, μAh)				
		1st complete cycle	2nd cycle	8th cycle	13th cycle	22nd cycle
Full cell open electrolyte	34.0 (0.21)	89.7 (142)	98.9 (157)	100 (159)	103 (163)	
Battery, packaged, in glove box	34.0 (0.21)	101 (159)	103 (163)	105 (167)	103 (164)	103 (163)
Battery, packaged, ambient conditions	34.0 (0.21)	98.0 (155)	98.3 (156)	97.8 (155)		

[a] The capacities are specified based upon the mass of $LiCoO_2$ in the battery system. The electrode areas are 4 mm × 4 mm.

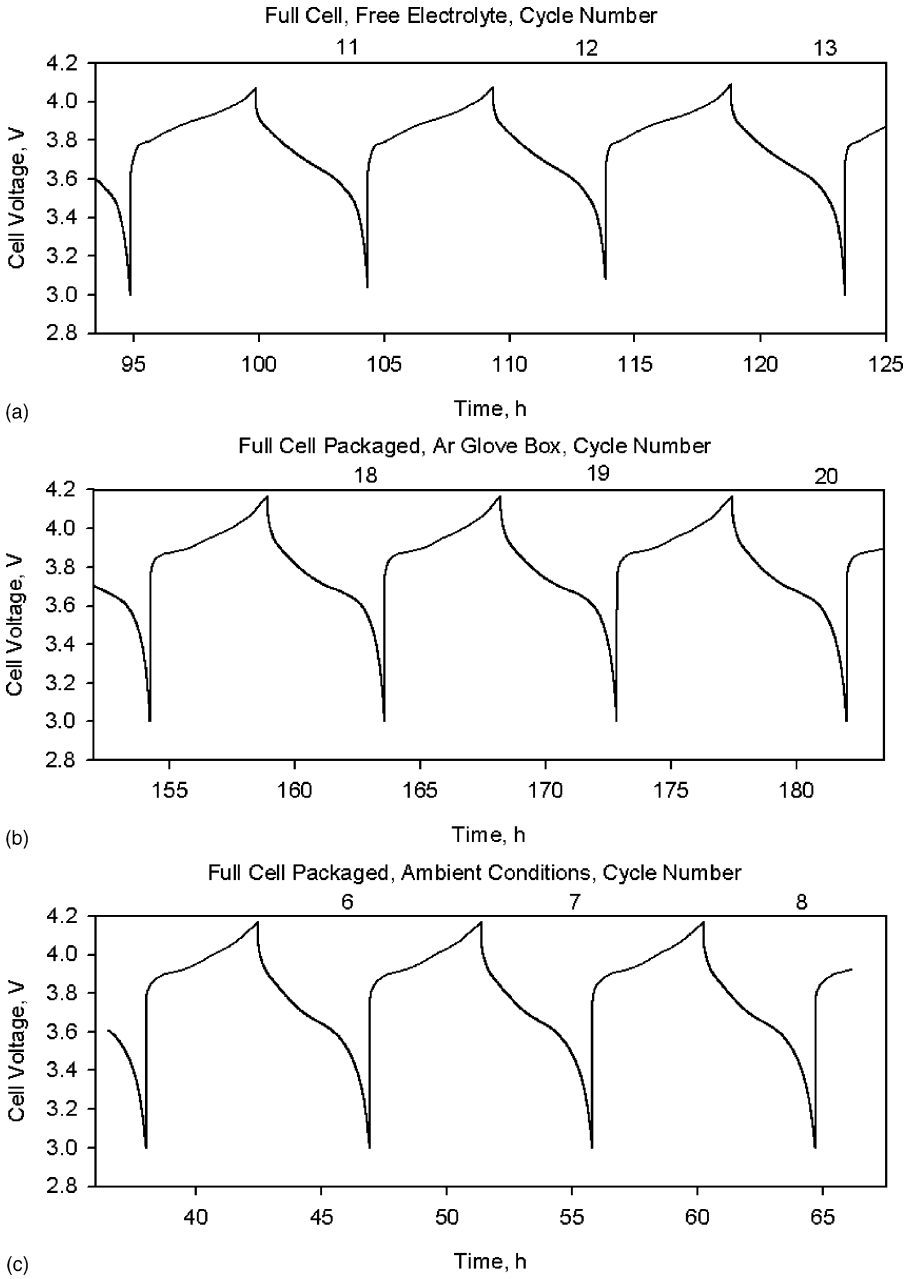

Fig. 5. Charge and discharge profiles of a pair of laser-transferred electrodes in 1 M $LiPF_6$/carbonate at different stages in the assembly of a microbattery: (a) cycles 11–13 of a full cell in open electrolyte in an Ar glove box; (b) cycles 18–20 of an encapsulated microbattery in an Ar glove box; (c) cycles 6–7 of the same encapsulated battery in ambient conditions. This experiment utilizes the same electrodes as those shown in Figs. 3 and 4 and the capacities are summarized in Table 2. The battery cycle number is reset to zero when the electrodes are moved to a new test condition.

a microbattery and packaged. Lastly, Fig. 5c shows the operation of the same micro-battery outside the Ar glove box and exposed to ambient conditions. After the first cycle in all cases, the microbattery has an approximate discharge capacity of 100 mAh/g_{LiCoO_2}. Therefore, the half-cell capacity of $LiCoO_2$ is maintained in the cell throughout the microbattery assembly process. Cells have an ohmic voltage drop of approximately 100 mV and their discharge plateaus end near 3.6 V. The discharge plateau becomes steeper as the electrodes are moved from the open electrolyte to the packaged cell and then to the open air in Fig. 5a–c, respectively. The increase in discharge slope may be due to a variety of changes experienced by the battery as it is transferred from open electrolyte into the packaged cell, the full analysis of which is beyond the purpose of this communication.

To show that the electrodes do not need to be cycled in half cells before assembly into a microbattery, electrodes have been assembled directly after drying in the vacuum oven. The electrodes are matched based upon their mass and assumed absolute capacity. Fig. 6a shows the charge

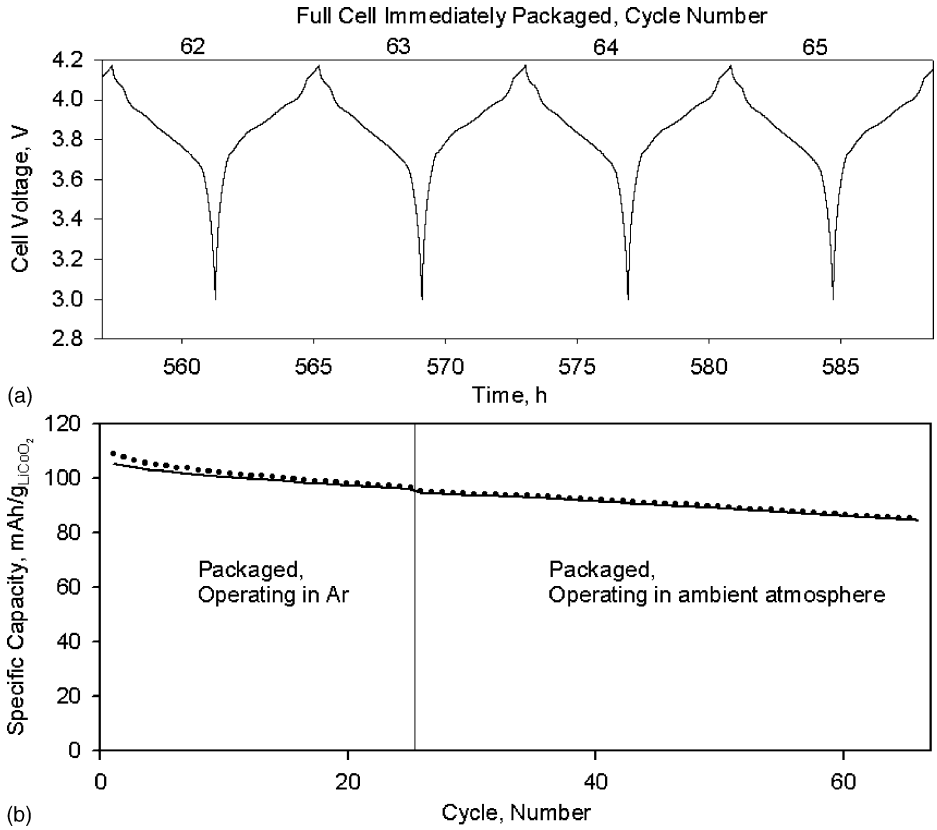

Fig. 6. An encapsulated microbattery prepared from electrodes that are not pre-cycled in half cells or open electrolyte: (a) charge and discharge profiles for cycles 62–65 in an Ar glove box; (b) the specific capacity of the cell under the Ar glove box and ambient atmosphere, where the circles are taken from charge data and the solid line from discharge data.

and discharge profiles for cycles 62–65 of the cell when operating in ambient conditions while Fig. 6b shows the specific capacity data, normalized to the mass of $LiCoO_2$, for the performance of the cell in an inert and then ambient environments. The first 25 cycles are performed in an Ar glove box, and they provide an average charge capacity of 102 mAh/g_{LiCoO_2} and average discharge capacity of 99.9 mAh/g_{LiCoO_2}, with an average decrease of 0.37% per cycle. Cycles 26–66 are performed under ambient conditions and only decrease by an average of 0.26% per cycle with an average charge capacity of 90.6 mAh/g_{LiCoO_2} and average discharge capacity of 89.8 mAh/g_{LiCoO_2}.

4. Discussion

The data presented in this paper demonstrate the capabilities of a laser direct-write process to make electrodes for Li-ion microbatteries. Comparison of laser-transferred electrodes with control electrodes in half-cell measurements shows that the laser interaction is not detrimental to the materials activity, allowing the use of materials that have already been optimized for commercial battery products (e.g. $LiCoO_2$ and MCMB). The control and laser-transferred carbon electrodes have capacities of 100–180 mAh/g_{Carbon} which is lower than the expected 300 mAh/g capacity of MCMB 25–28. However, the similarity between the capacity of the laser-transferred and control electrodes indicates that factors other than the laser transfer, such as electrode or cell geometry [19], are responsible for non-theoretical behavior. The capacity of the laser-transferred carbon electrodes might be improved by optimizing the carbon powder packing and/or carbon particle size distribution [20]. The particle packing of the electrode pads may be changed by modification of the direct-write process parameters (e.g. varying the flight distance from the ribbon to the substrate, the concentration of the organic vehicle, and the curing of the PVDF binder).

The microbatteries assembled from laser-transferred electrodes have properties that are comparable to those fabricated using sputtering. The sputter-deposited microbatteries of Bates et al. [5], which have a 1 cm^2 footprint and a 2.5 μm thick $LiCoO_2$ layer, have capacities of 156 μAh or 62.4 μAh/(cm^2 μm_{LiCoO_2}) at an interpolated current density of 0.2 mA/cm^2 and a $LiCoO_2$ density of 5.06 g/cm^3 [21]. In comparison, the laser-transferred 40 μm × 0.16 cm^2 positive electrode detailed in Table 2 has a capacity of 155 μAh or 24.2 μAh/(cm^2 μm_{LiCoO_2}) at a current density of 0.2 mA/cm^2 and a $LiCoO_2$ density of 2.48 g/cm^3. The sputtered $LiCoO_2$ electrodes have twice the density of the

laser-transferred positive electrodes because the films are sintered after sputtering and do not contain any additives (carbon or binder), and therefore have higher volumetric capacity than the laser direct-write electrodes. However, the laser-transferred electrodes have lower resistivity than sputtered electrodes because they contain carbon, so they can be made thicker without creating a significant IR drop. The laser-transferred electrodes therefore can occupy a smaller footprint than the sputtered ones (0.16 cm^2 for a 155 μAh laser-transferred microbattery vs. 1 cm^2 for a 156 μAh sputtered microbattery).

The first generation of Li-ion microbatteries described in this manuscript are stand-alone units that can be used as surface-mount components in devices. Next steps require improvement of the separator/electrolyte, current collectors, and encapsulation materials. A high conductivity solid electrolyte/separator may be formed from a porous layer of oxide or phosphate nanoparticles [22]. Laser direct-write processes have been devised for copper [23] and aluminum [24] films, and these methods may be adopted to create current collectors. Palladium lines can also be deposited by laser direct-write [25] to serve as interconnects. Low-temperature melting glasses can be laser densified [26] to form air-tight encapsulation. By combining the laser-transferred electrodes demonstrated herein with these other fabrication tools, it may be possible to directly integrate high capacity, lightweight microbatteries into microdevices and microsensors for autonomous deployment.

5. Summary

A laser direct-write process is demonstrated as a promising approach for fabricating Li-ion microbattery electrodes. Composite powders of $LiCoO_2$, carbon and binders are laser-forward transferred onto laser-micromachined metal foils. The laser-deposited $LiCoO_2$-positive and carbon-negative electrodes have similar capacities to control electrodes that are stenciled and then pressed. Therefore, the laser interaction with the materials is not detrimental to their activity. The electrodes are tested in half-cell configurations to determine their capacities. Electrodes with matching capacities are paired in full-cell configurations in an excess of open electrolyte, before assembling them as an encapsulated microbattery and testing in ambient conditions. Microbatteries have also been assembled from freshly prepared electrodes (that were not first cycled in half cells) to demonstrate the feasibility of a sequential production process. A microbattery with a 4 mm × 4 mm electrode footprint, 40 μm thick $LiCoO_2$ composite positive electrode, and 60 μm thick carbon composite negative electrode has an absolute capacity of 155 μAh and a specific capacity of 97.8 mAh/g (based upon the 1.585 mg mass of $LiCoO_2$). These 0.16 mm^2 laser direct-write cells have a similar capacity to 1 mm^2 sputtered thin-film Li-ion cells. Although the laser direct-write microbatteries have less volumetric capacity than the sputtered microbatteries, they can be made thicker and thus use a smaller footprint to deliver the same capacity. Laser direct-write methods are demonstrated to be viable for making Li-ion microbattery electrodes, which is the first step in building an integrated microbattery with a microelectronic device.

Acknowledgements

The authors thank the Office of Naval Research for supporting this research. RW is a postdoctoral associate with the American Society for Engineering Education, and AEC and CBA are postdoctoral associates with the National Research Council.

References

[1] K.E. Swider-Lyons, A. Piqué, C.B. Arnold, R.C. Wartena, in: Q.M. Zhang, E. Fukada, Y. Bar-Cohen, S. Bauer, D.B. Chrisey, S.C. Danforth (Eds.), Electroactive Polymers and Rapid Prototyping, Materials Research Society Proceedings Series, vol. 698, Materials Research Society, Warrendale, PA, USA, 2002, p. 265.
[2] J.N. Harb, R.M. LaFollette, R.H. Selfridge, L.L. Howell, J. Power Sources 104 (2002) 46–51.
[3] S. Roundy, P.K. Wright, J. Rabaey, Comp. Commun. 26 (2003) 1131–1144.
[4] S.D. Jones, J.R. Akridge, Solid State Ion. 86–88 (1996) 1291–1294.
[5] J.B. Bates, N.J. Dudney, B. Neudecker, A. Ueda, C.D. Evans, Solid State Ion. 135 (2000) 33–45.
[6] W.C. West, J.F. Whitacre, V. White, B.V. Ratnakumar, J. Micromech. Microeng. 12 (2002) 58–62.
[7] B.J. Neudecker, R.A. Zuhr, J.B. Bates, J. Power Sources 81–82 (1999) 27–32.
[8] S.-H. Lee, P. Hu, C.E. Tracy, D.K. Benson, Electrochem. Solid State Lett. 2 (9) (1999) 425–427.
[9] K. Kushida, K. Kuriyama, T. Nozaki, Appl. Phys. Lett. 81 (26) (2002) 5066–5068.
[10] P.H. Humble, J.N. Harb, R. LaFollette, J. Electrochem. Soc. 148 (2001) A1357–A1361.
[11] A. Piqué, D.B. Chrisey (Eds.), Direct-write Technologies for Rapid Prototyping Applications, Academic Press, San Diego, 2002.
[12] A. Piqué, D.B. Chrisey, R.C.Y. Auyeung, J. Fitz-Gerald, H.D. Wu, R.A. McGill, S. Lakeou, P.K. Wu, V. Nguyen, M. Duignan, Appl. Phys. A 69 (Suppl.) (1999) S279–S284.
[13] A. Piqué, D.B. Chrisey, J.M. Fitz-Gerald, R.A. McGill, R.C.Y. Auyeung, H.D. Wu, S. Lakeou, V. Nguyen, R. Chung, M. Duignan, J. Mater. Res. 15 (2000) 1872–1875.
[14] A. Piqué, R.C.Y. Auyeung, J.L. Stepnowski, D.W. Weir, C.B. Arnold, R.A. McGill, D.B. Chrisey, Surf Coat. Technol. 163 (2003) 293–299.
[15] C.B. Arnold, R. Wartena, K.E. Swider-Lyons, A. Piqué, J. Electrochem. Soc. 150 (2003) A571–A575.
[16] R. Wartena, C.B. Arnold, A. Piqué, K.E. Swider-Lyons, in: E.J. Brandon, A. Ryan, J. Harb, R. Ulrich (Eds.), MicroPower and MicroDevices, The Electrochemical Society Proceedings Series, PV 2002-25, Electrochemical Society, Pennington, NJ, USA, 2002, p. 16.
[17] D. Terzidiz, C.L. Mitsas, E. Hatzikraniotis, I. Papadopoulos, T. Zorba, G. Moumouzias, D.I. Siapkas, S. Kokkou, Solid State Ion. 135 (2000) 297–304.
[18] D. Linden, T.B. Reddy (Eds.), Handbook of Batteries, 3rd ed., McGraw-Hill, New York, 2001.

[19] P.H. Humble, J.N. Harb, J. Electrochem. Soc. 150 (2003) A1182–A1187.
[20] Y. Sato, T. Nakano, K. Kobayakawa, T. Kawai, A. Yokoyama, J. Power Sources 75 (1998) 271–277.
[21] P.J. Bouwman, B.A. Boukamp, H.J.M. Bouwmeester, P.H.L. Notten, J. Electrochem. Soc. 149 (2002) A699–A709.
[22] P. Birke, F. Salam, S. Doring, W. Weppner, Solid State Ion. 118 (1999) 149–157.
[23] C.M. Harish, V. Kumar, A. Prabhakar, Semiconduct. Manuf. IEEE Trans. 6 (1993) 279–282.
[24] H.W. Lee, S.D. Allen, Appl. Phys. Lett. 58 (1991) 2087–2089.
[25] M.E. Gross, A. Applebaum, P.K. Gallagher, J. Appl. Phys. 61 (1987) 1628–1632.
[26] C.S. Sandu, V.S. Teodorescu, C. Ghica, B. Canut, M.G. Blanchin, J.A. Roger, A. Brioude, T. Bret, P. Hoffmann, C. Garapon, Appl. Surf. Sci. 208–209 (2003) 382–387.